PROCESS MODELING OF A CLOSED-LOOP SCO_2 GEOTHERMAL POWER CYCLE

Brian S. Higgins†
Mark P. Muir
Alan D. Eastman

GreenFire Energy
4300 Horton Ave, Unit 15
Emeryville, CA 94608

Curtis M. Oldenburg
Lehua Pan

Energy Geosciences Division 74-316C
Lawrence Berkeley National Laboratory
Berkeley, CA 94720

ABSTRACT

A closed-loop geothermal power cycle has been designed and optimized for power production using supercritical CO_2 as the working fluid. Since it is closed loop, heat extraction from the resource to the well is by conduction. The sCO_2 that is returned to the surface is used to directly produce power, then cooled and reinjected to complete the cycle. This paper reviews the process modeling, including a simple 1D explicit solution of the mass and energy conservation equations, utilizing a semi-empirical conduction relationship to capture the time-resolved depletion of the geothermal resource. A second 3D model is used containing mixed convective-conductive fluid-flow modeling with the T2Well/TOUGH2 wellbore flow model to investigate the critical factors that control closed-loop geothermal energy recovery. T2Well solves a mixed explicit-implicit set of momentum equations for flow in the pipe with full coupling to the implicit 3D integral finite difference equations for Darcy flow in the porous medium.

As a result of these modeling studies, we find that for each resource and well geometry, there is an optimum tradeoff between power produced and the mass flow of sCO_2. At a moderately low flow of sCO_2, a strong thermosiphon develops and the production temperature is highest, however the power production is relatively low. As the sCO_2 flow rate is increased, the thermosiphon weakens due to friction in the well and the production temperature decreases because the rate of heat extraction is limited by heat transfer from the resource and not by the extraction potential of the sCO_2. Through parametric analysis using these models, it is possible to determine the process conditions that maximize power output. The modeling results suggest that the thermosiphon accounts for a large portion of this maximized power output, thermal degradation is modest, and that moderate levels permeability and convection do not substantially increase power production, but very high levels of permeability do provide for a substantial power increase.

† Brian.Higgins@GreenFireEnergy.com

INTRODUCTION

Despite the enormous, worldwide potential of geothermal energy, only a small fraction of the recoverable geothermal heat can be retrieved with conventional hydrothermal technology (Tester et al., 2006). Conventional hydrothermal power production requires a natural combination of heat, subsurface permeability, and abundant water. This leaves undevelopable the vast majority of hot geothermal resources that have relatively non-permeable rock. Even when all three requirements are present, exploration risk (i.e., dry holes) leads to wells drilled at great cost that cannot be productively used. Also, while conventional hydrothermal operations attempt to maintain the flow of water in the formation and avoid excessive cooling of the resource, the performance of typical hydrothermal operations degrade over time, sometimes rapidly. Further challenging conventional hydrothermal power are environmental challenges such as water pollution and surface subsidence. Water produced from hydrothermal reservoirs often contains high levels of dissolved chemicals that can cause problems within the power producing equipment (e.g., scaling and corrosion) or can result in emissions (e.g., acid gases and CO_2, a greenhouse gas). Removal of these dissolved chemicals can require costly treatment. We believe that all of these problems can be avoided by using a closed-loop circulation system, where the working fluid never comes in contact with the rock.

ECO2G TECHNOLOGY

Conventional geothermal technologies obtain geothermal brine from fractures in rock formations and therefore require permeable rock and large quantities of water, which require high-pressure pumps. GreenFire Energy's ECO2G™ technology, in contrast, circulates supercritical CO_2 through a closed-loop well system. It is viable at locations that do not have permeability or abundant water, which makes up the majority of known resources. Vastly larger geothermal areas thus become available for exploration and the risk and time to permit usually associated with geothermal projects is drastically reduced.

Supercritical CO_2 was selected as the working fluid for several reasons. The formation of a thermosiphon is a key attribute, but many refrigerants will also form a thermosiphon. Supercritical CO_2 is highly compressible and has a large capacity for heat absorption near its critical point. Supercritical CO_2 is relatively inexpensive compared to other refrigerants. It is also relatively inert and will not react with the well, turbine, or the heat exchanger materials of construction. Supercritical CO_2 turbines are available, which are relatively low cost, robust, high performance, fairly small, and require little maintenance. Due to the relatively low temperature and pressure of the critical point (31°C, 7.4 MPa), the use of sCO_2 can significantly reduce or even eliminate the need for process water, though this is very site specific.

The sCO_2 thermodynamic cycle outperforms water with a flash tank in terms of both power and power density, when equivalent process cycles are compared.

THERMODYNAMIC CYCLE

The normal gas path through a Brayton cycle comprises the following steps: compression, heat addition through a recuperator, heat addition by a heat source, high-pressure expansion, reheating, low-pressure expansion, heat rejection through the recuperator, heat rejection to the heat sink, and then recirculation back to the compression stage.

For a geothermal gas cycle, a recuperator can only be placed before or after the well. Placing it after the well is unproductive, since this would require additional heat to be added over and above the geothermal heat. Placing a recuperator before the well would heat up the sCO_2 before it enters the injection well, reducing or completely eliminating the thermosiphon. Reheating also makes little sense since it would involve drilling a second well. Finally, in the absence of a recuperator, there is no benefit to over-expanding the sCO_2 at the exit of the turbine and then recompressing it before reinjecting it into the ground.

The net effect of these factors is that a sCO_2 thermodynamic cycle for closed-loop geothermal energy is quite simple. There are only two required above-ground process steps: expansion and heat rejection. Compression can be used in place of turbine controls (e.g., pressure ratio), but is not required since the downhole pressure can be balanced by simply changing the volume of sCO_2 in the process loop.

PROCESS MODELING

We have built and optimized a 1D process model that takes into account conservation of mass and energy. The governing physics for the process model includes isentropic compression and expansion as the sCO_2 moves up or down the well. Friction is accounted for in the well using a Darcy friction factor via the Haaland equation (Haaland, 1983). Friction manifests itself in the model as pressure drop in the flow of sCO_2 through the well. Heat transfer is modeled as 1D conduction everywhere except between the casing and the flowing sCO_2, which is modeled as convection using a Nusselt number calculated with the Dittus-Boelter equation (Bergman, 2011). Time-resolved conduction through the resource is modeled using the semi-empirical Ramey correlation (Ramey, 1962). Convection through the resource is not considered in the 1D model. The 1D model results compare favorably to results from the 3D model (described below) for the 3D case where the resource has very low permeability.

The above-ground surface equipment comprises a turbine, heat exchanger, and optional compressor. The turbine and compressor are modeled using a specified isentropic turbine efficiency assumption. The heat exchanger can be modeled as either a gas-gas heat exchanger or as an evaporative water-cooling system. Heat rejection, in either case, is heavily dependent on the ambient weather conditions, so this is also considered in the process modeling.

3D MODELING METHODS

Simulations of the closed-loop system are carried out using a member of the TOUGH (Pruess et al., 2010; 2012) family of codes called T2Well (Pan et al., 2011; Pan and Oldenburg, 2014). T2Well models flow in the wellbore by solving the 1D transient momentum equation of the fluid mixture with the drift-flux model (DFM), and flow in the reservoir using the standard multiphase Darcy's law equation. Because we consider pure sCO_2 in the pipe above the critical pressure, we effectively have single-phase flow. The geothermal system outside the pipe is assumed to be a liquid-dominated geothermal system (i.e., pure water in aqueous phase). Because the sCO_2 is isolated from the reservoir by the well casing, there is no advective coupling between the pipe and the reservoir. This is a greatly simplified system compared to the two-phase (CO_2-rich and H_2O-rich) wellbore-reservoir coupling processes that T2Well is capable of modeling (e.g., Oldenburg et al., 2012; Oldenburg and Pan, 2013). For single-phase conditions in the pipe, the transient momentum equation of sCO_2 pipe flow, including temporal momentum change rate, spatial momentum gradient, friction loss to the pipe wall, gravity, and pressure gradient are solved to obtain the velocity of flowing sCO_2. In the reservoir, natural convection may occur depending on the permeability, which limits it and the buoyancy, which drives it. We use ECO2N V 2.0 (Pan et al., 2014) to model the thermophysical properties of sCO_2 and water. Grid generation is carried out using WinGridder (Pan, 2003).

PROCESS DESIGN

Once the 1D model was developed and was shown to produce results consistent with the 3D model for analogous inlet and outlet conditions and with low permeability in the reservoir, various design parameters were parametrically tested using each of the models separately. These parameters include:

1) Well diameter, length, and depth
2) Cement parameters (i.e., thickness and thermal conductivity)
3) Well configuration (described below)
4) Geothermal resource properties (e.g., temperature, density, and specific heat as a function of depth

For any given well parameter, the sCO_2 flow rate was varied in the model to find the optimum flow to maximize power. The full process modeling campaign considered over 50,000 different combinations of the above parameters. Typical results showing variable sCO_2 flow rates for one parametric case are presented in Figure 1. In comparing results between the 1D and 3D models, it should be noted that the outlet end of the pipe in the 3D model was held at fixed pressure, while the inlet flow rate was specified. In contrast, for the 1D model a fixed inlet pressure is assumed.

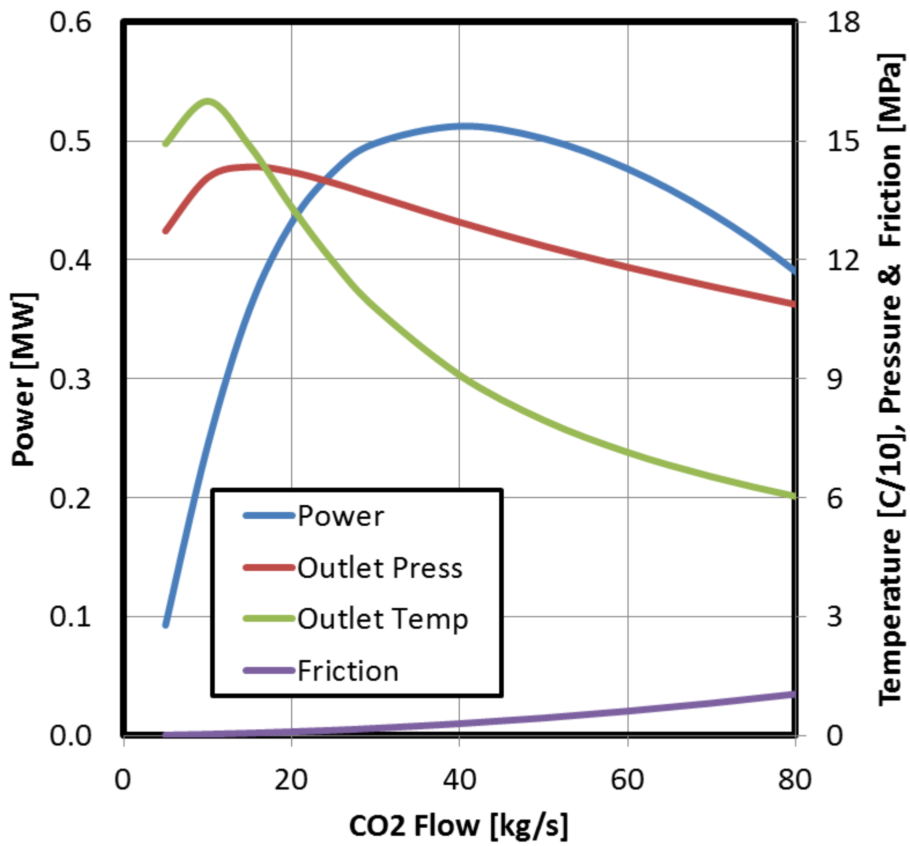

Figure 1: Power, outlet pressure, outlet temperature, and friction are plotted versus the flow of sCO_2, showing that there is a maximum in the power produced, representing a tradeoff between friction and resource heat extraction.

Considering the data in Figure 1, when the sCO_2 flow rate is relatively low, both the production temperature and pressure are highest; however the power produced is low. This is because high production temperature and pressure mean that the production gas has high specific enthalpy, but the overall enthalpy extracted from the well is low, and even with a high efficiency turbine the overall power produced is low. As the sCO_2 flow rate is increased, both the produced pressure and temperature drop. The pressure drops because of increased effects of friction in the well and density changes, and the temperature drops due to the limit of how much heat can be extracted from the resource; nevertheless, the power increases due to higher mass flow. However, as the sCO_2 flowrate is further increased, the power eventually starts to decrease due to a large drop in the thermosiphon (produced pressure) and lower relative heat absorption (produced temperature). The maximum power thus is a function of the balance between lower flows that produce a higher thermosiphon and higher production temperatures and higher flows that have increased friction and lower production temperatures. This is relationship was found to be true for all parametric conditions tested.

CONFIGURATIONS

Various well configurations have been proposed to isolate the formation rock and geothermal brine from the working fluid used to recover energy. Examples include single wells where the working fluid both enters and exits the same hole, connected wells where the working fluid enters and leaves different wells that are connected at the bottom into a continuous loop, and multiplexed wells where there may be multiple entrances, exits, or passages underground.

In this study, we consider a U-shaped configuration with a significant horizontal portion to increase contact with the high-temperature reservoir, schematically represented in Figure 2.

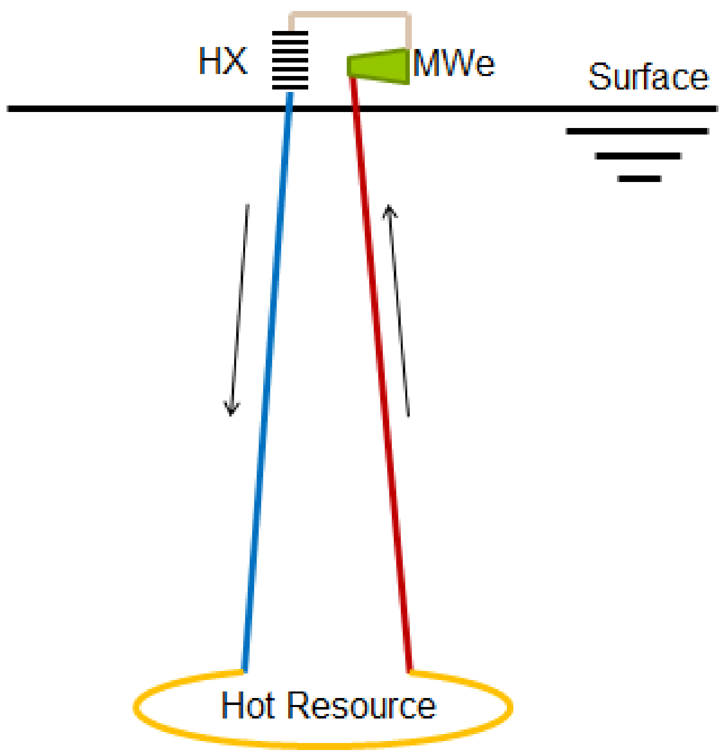

Figure 2: Sketch of closed-loop geothermal energy system for sCO_2 flowing counterclockwise in the figure, including the injection well (blue), horizontal section (yellow), production well (red), turbine (green), and heat rejection (HX).

Figure 2 schematically represents the studied well configuration, which is topologically the same as a “U”. It makes no difference to the modeling if the injection well is close to, or far from, the location of the production well. Similarly, the model does not consider whether the horizontal section (yellow) is curved or not. The transition between the vertical sections (blue and red) and the horizontal section (yellow) is also not addressed in the model and, in reality, would gradually transition from vertical to horizontal over several hundred meters.

RESULTS

The process modeling results are presented for the 1D modeling case first, and then for the 3D modeling case second.

1D Process Modeling Results Summary

The focus of the 1D modeling for this paper was optimizing the thermodynamic cycle for the production of power for one specified well configuration and resource.

In Figure 3, the T-s diagram is presented for the optimized cases. The inlet conditions of the sCO_2 are at the bottom left of the process loop (bottom of the blue line), where the properties are near the critical point of sCO_2 (T_c = 31°C and P_c = 7.4 MPa). The orange line represents the subcritical vapor dome.

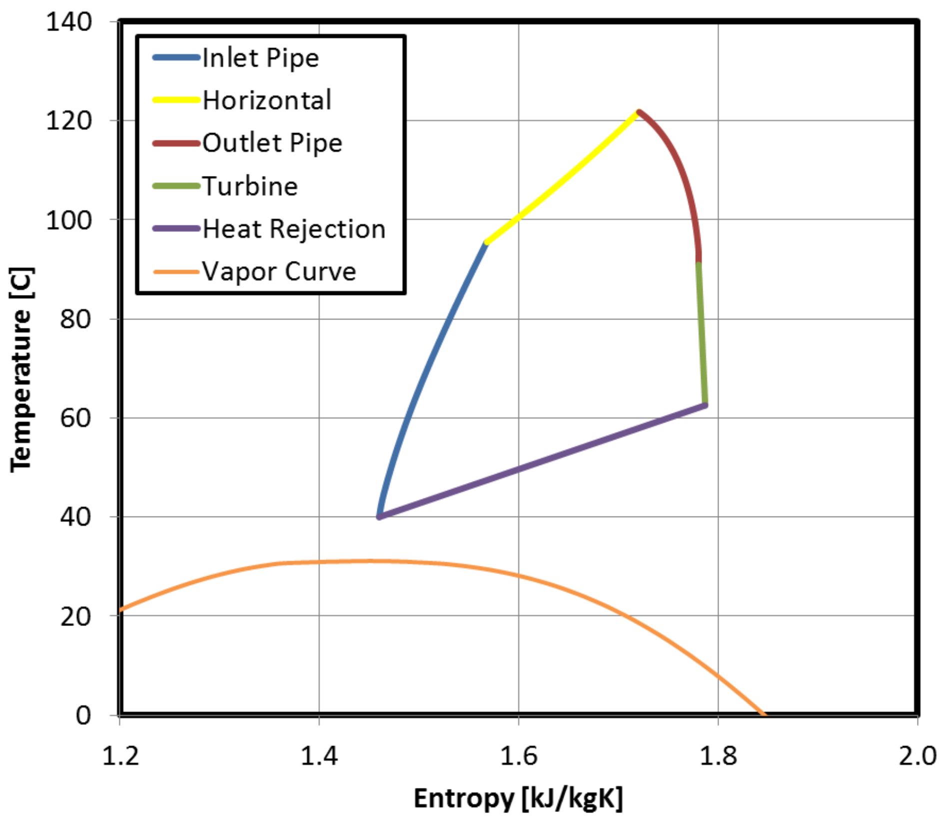

Figure 3: T-s Diagram: Temperature plotted versus specific entropy with sCO_2 flowing counterclockwise in the figure and shows the injection well (blue), horizontal section (yellow), production well (red), turbine (green), and heat rejection (HX).

Following the blue line Figure 3 from bottom to top, the sCO_2 increases in temperature as it flows down the injection pipe due to isentropic compression. Initially the line is more vertical since not as much heat is being absorbed from the resource. As the sCO_2 reaches the bottom of the well, where the resource is hot and heat is being absorbed by the sCO_2, the blue line bends to the right, indicating entropy increase due to heat transfer, and not just due to compression.

When the sCO_2 reaches the horizontal section (yellow line), it continues to gain temperature, but now only by heat transfer. This increases both the temperature and the entropy. Finally, the sCO_2 starts to move up the production well (red line) and while it is still cooler than the resource and is still absorbing heat, it is also expanding and losing temperature due to adiabatic expansion. This continues until the entrance of the turbine (green line), where power is produced by the produced enthalpy. The slight slope of the green line to the right depicts the inefficiency of the turbine. The purple line along the bottom represents the heat rejection that occurs across the heat exchanger, required to return the sCO_2 back to the starting thermodynamic state.

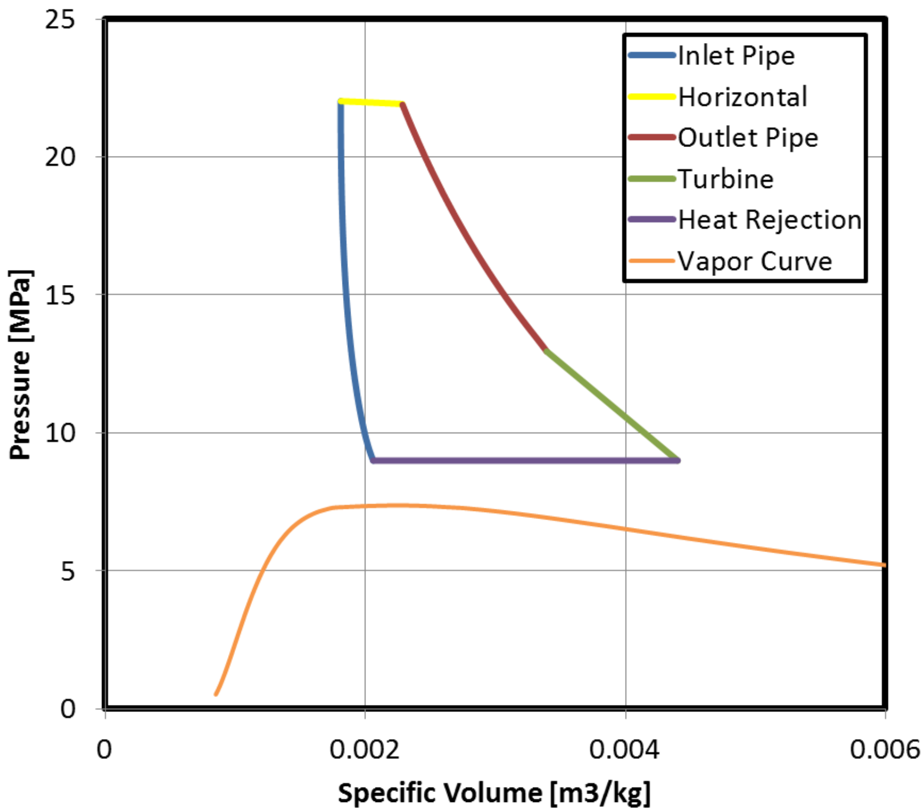

Figure 4: P-v Diagram: Pressure plotted versus specific volume with sCO_2 flowing counterclockwise in the figure and shows the injection well (blue), horizontal section (yellow), production well (red), turbine (green), and heat rejection (HX).

In Figure 4, the P-v diagram is presented. The inlet conditions of the sCO_2 are again at the bottom left of the process loop (bottom of the blue line), near the critical point. As the sCO_2 flows down the injection well, the pressure builds up and the density is increased (density equals the inverse of specific volume). The increase in density occurs even as the sCO_2 is increasing in temperature (compare with Figure 3). Once the sCO_2 turns the corner to the horizontal section, the pressure stays nearly the same and the density decreases to less than the injection density, even while at substantially increased bottom-hole pressure. As the sCO_2 starts moving up the production well, the pressure is reduced substantially, resulting in a large density change. The column weight difference due to this density change between the injection well and the production well produces the thermosiphon. The exit of the production well shows significantly more pressure than the entrance to the injection well. This pressure increase, combined with the temperature increase (shown in Figure 3) equates to an enthalpy increase, which is directly used to generate power by the sCO_2 turbine. The turbine exit pressure is the same as the injection pressure, and therefore, no compression is required.

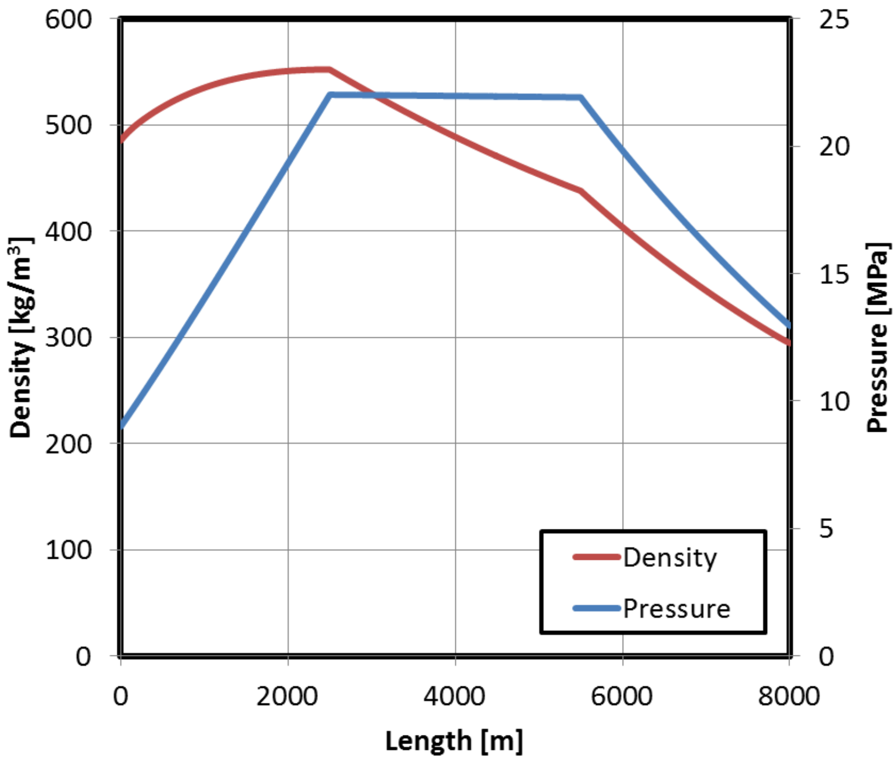

Figure 5: Plot of pressure (blue) and density (red) as a function of distance from the injection well, demonstrating the thermosiphon.

The effect of sCO_2 density change and its effect on the thermosiphon are shown directly in Figure 5. The red line represents sCO_2 density as it flows through the well. The first third of the red line is the injection well, where the density averages much higher than in the last third of the red line, which is the production well. This density differential produces the pressure difference shown as the relative change in the blue line from left to right in Figure 5. As shown by the blue line, the sCO_2 exits the production well (right side of figure) at a substantially higher pressure than is present at the injection well (left side of figure).

3D Modeling Results Summary

For the 3D modeling, results are presented for several cases similar to the results above. Many more modeling details, results, and conclusion from the 3D modeling effort can be found in our longer 3D modeling focused paper (Oldenburg et al., 2016).

As sCO_2 flows down the well into hot regions of the subsurface, its energy changes as it loses gravitational potential, heats up by compression and by absorbing heat through the hot pipe wall, and as its velocity changes. These four forms of energy - pressure-volume, thermal, kinetic, and gravitational potential - are all accounted for in T2Well in the output energy gain (MW). We note that because mass is conserved in the pipe and the inlet is at the same elevation as the outlet, the gravitational potential energy difference across the system is always zero.

In Figure 6a, results are shown for energy gain for three cases: Case 1 with negligible reservoir permeability (low-k), Case 2 with low permeability (standard-k), and Case 3 with high permeability consistent with stimulation around the wellbore (high-k). The low-k and standard-k cases (Cases 1 and 2) both produce about 1.75 MW at nearly steady state for the modeled conditions. In the low-k case (Case 1), convection is negligible in the reservoir. The small differences between the first two cases show that convective heat transfer is negligible when the reservoir has permeability less than 1 Darcy. On the other hand, Case 3, with a high-k zone around the well, produces about twice as much energy as Cases 1 and 2 and demonstrates that high natural convection in the reservoir can greatly enhance energy recovery.

We note also in Figure 6a that the thermal resource is not appreciably depleted over the 30 years of simulation. The model has a constant-temperature boundary condition at the bottom that serves to replenish heat. For Case 3 with a highly stimulated near-well region, Figure 6a shows that the energy gain declines over time as local convective heat transfer to the pipe appears to exceed the conductive heat transfer into the near-well region needed to replenish extracted heat.

(a)

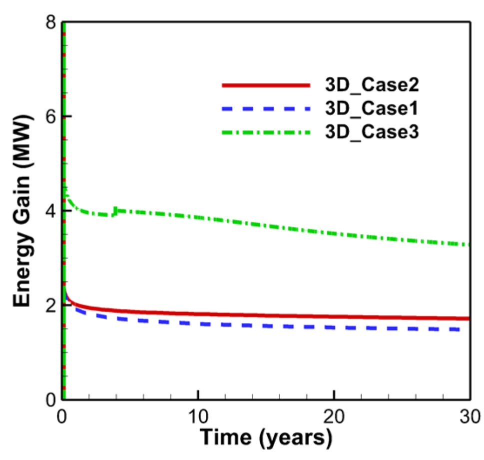

(b)

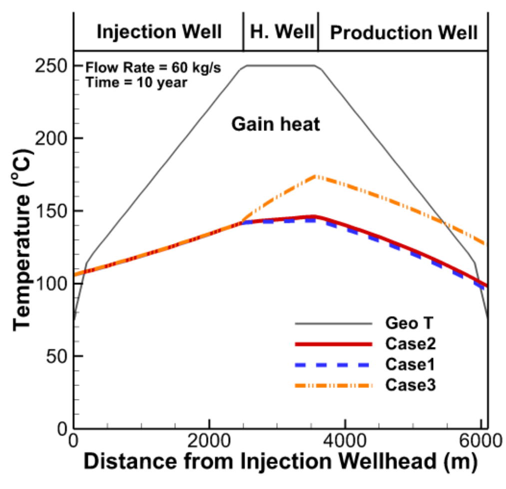

Figure 6: Simulation results of the effect of reservoir permeability on energy gain in the closed loop. (a) High-permeability in the reservoir favors convective heat transfer to the pipe. (b) The effects of convective heat transfer to the pipe are largest in the horizontal section of the closed loop.

Temperature along the well is shown for the three cases in Figure 6b. The temperature profile "Geo T" represents the geothermal resource temperature. When sCO_2 is injected the temperature in the well is lower than the initial temperature everywhere except near the tops of the inlet and outlet sides of the well. This shows that there is potential for heating of the sCO_2 all along the well except at shallow depths near the inlet and outlet points[‡]. The data for Case 3 in this figure demonstrate the strong benefit of the convective heat transfer that occurs if the near-well region can be stimulated to support natural convection.

CONCLUSIONS

We have used a 1D process design model to determine the process flow conditions for a supercritical CO_2 closed-loop power cycle without taking into account the effects of permeability in the geothermal formation. The process design results show that the thermosiphon contributes importantly to the power produced, and that power production can be maximized by optimizing the flow of sCO_2 through the system even for resources without significant permeability. We have also performed a 3D model using a detailed coupled pipe-reservoir model to investigate the effects of various parameters on the energy gain of sCO_2 flowing in a U-shaped well through a geothermal reservoir. While convection from moderate reservoir permeability was shown to not significantly increase energy gain, convection in highly permeable resources was shown to provide substantial energy gains. The 3D model also showed that thermal depletion was very modest of the 30 years modeled and not significantly dependent on permeability of the geothermal resource. Variables considered included pipe diameter, well depth, horizontal well length, temperature gradients, flow rates, and pressures.

[‡] In general, at shallow depths up to several km, a well will have several overlapping casings with several layers of cement. This is not modeled. If these were modeled, the heat loss at shallow depths would be reduced, leading to a prediction of increased heat extraction.

REFERENCES

Bergman, Theodore L., Frank P. Incropera, and Adrienne S. Lavine. Fundamentals of heat and mass transfer. John Wiley & Sons, (2011).

Haaland, S.E. Simple and explicit formulas for the friction factor in turbulent pipe flow. Journal of Fluids Engineering, 105(1), 89-90 (1983).

Oldenburg, C.M., and L. Pan, Porous Media Compressed-Air Energy Storage (PM-CAES): Theory and Simulation of the Coupled Wellbore–Reservoir System, *Transport in Porous Media*, *97*(2) 201-221 (2013).

Oldenburg, C.M., B.M. Freifeld, K. Pruess, L. Pan, S. Finsterle, and G.J. Moridis. Numerical simulations of the Macondo well blowout reveal strong control of oil flow by reservoir permeability and exsolution of gas. *Proceedings of the National Academy of Sciences 109*, no. 50: 20254-20259 (2012).

Oldenburg, C.M., L. Pan, M.P. Muir, A.D. Eastman, and B.S. Higgins. Numerical Simulation of Critical Factors Controlling Heat Extraction from Geothermal Systems Using a Closed-Loop Heat Exchange Method. *Proceedings of the 41st Workshop on Geothermal Reservoir Engineering*, SGP-TR-209, Stanford University, Stanford, California, February 22-24 (2016).

Pan, L., C.M. Oldenburg, Y. Wu, and K. Pruess, T2Well/ECO2N Version 1.0: Multiphase and Non-Isothermal Model for Coupled Wellbore-Reservoir Flow of Carbon Dioxide and Variable Salinity Water, Lawrence Berkeley National Laboratory Report *LBNL-4291E* (2011).

Pan, L., Spycher, N., Doughty, C. and Pruess, K., ECO2N V. 2.0: A New TOUGH2 Fluid Property Module for Mixtures of Water, NaCl, and CO_2. Ernest Orlando Lawrence Berkeley National Laboratory Report *LBNL-6930E*, Berkeley, CA (2014).

Pan, L., Wingridder-an interactive grid generator for TOUGH2. Lawrence Berkeley National Laboratory. Pan, L., and C.M. Oldenburg. "T2Well—An integrated wellbore–reservoir simulator." *Computers & Geosciences 65: 46-55* (2003).

Pruess, K., C.M. Oldenburg, and G.J. Moridis. TOUGH2 User's Guide Version 2. E. O. Lawrence Berkeley National Laboratory Report *LBNL-43134*, 1999; and *LBNL-43134* (revised) (2012).

Pruess, K., Enhanced geothermal systems (EGS) with CO_2 as heat transmission fluid--A scheme for combining recovery of renewable energy with geologic storage of CO_2. Lawrence Berkeley National Laboratory (2010).

Ramey Jr, H.J., Wellbore heat transmission. *Journal of Petroleum Technology*, *14*(04), pp.427-435 (1962).

Tester, J. W., Anderson, B., Batchelor, A., Blackwell, D., DiPippo, R., Drake, E., ... & Petty, S. The future of geothermal energy: Impact of enhanced geothermal systems (EGS) on the United States in the 21st century. Massachusetts Institute of Technology, 209 (2006).